# Experimental verification of broadband superlensing using a metamaterial with an extreme index of refraction

Mário G. Silveirinha,[1] Carla R. Medeiros,[2] Carlos A. Fernandes,[2] and Jorge R. Costa[2,3]
[1]*Department of Electrical Engineering, Instituto de Telecomunicações, University of Coimbra, 3030 Coimbra, Portugal*
[2]*Instituto de Telecomunicações–Instituto Superior Técnico, Av. Rovisco Pais, 1049-001 Lisboa, Portugal*
[3]*Instituto de Telecomunicações–Instituto Superior de Ciências do Trabalho e da Empresa, Av. das Forças Armadas, 1649-026 Lisboa, Portugal*

(Received 18 September 2009; revised manuscript received 16 November 2009; published 4 January 2010)

Here, we report the experimental realization of a flat near-field lens formed by an array of densely packed crossed metallic wires. It is shown that due to the unusually strong electric response of the inclusions, the metamaterial slab may enhance the deep subwavelength spatial spectrum of a given source. It is experimentally demonstrated that when the superlens is placed in between the source and the image planes, keeping the propagation distance in the air regions unchanged, the resolution is boosted by a factor of 2 over a broad bandwidth that may exceed 25% the frequency of operation.

DOI: 10.1103/PhysRevB.81.033101 PACS number(s): 42.70.Qs, 78.20.Ci, 41.20.Jb, 78.66.Sq

Imaging the tiny features of an object, beyond the possibilities offered by conventional optics, has become a topic of central importance after Pendry[1–6] suggested that by nanostructuring conventional dielectrics or metals it may be possible to manipulate light in a way beyond the reach of typical bulk materials. The original "perfect lens"[1] was based on materials with simultaneously negative permittivity and permeability. However, a similar superlensing effect can be observed in the near-field zone using materials with only an electric response ($\varepsilon \approx -1$, e.g., the "silver lens"),[2] or with only a magnetic response ($\mu \approx -1$),[3] or alternatively using photonic crystals.[7,8] The mechanism that enables the restoration of the near field in both the perfect lens and the silver lens is the excitation of guided modes (associated with surface-plasmon polaritons) at the interfaces of the flat lens,[1,2] which due to their characteristically short wavelengths along the direction of the interface can effectively probe the fine details of an object. However, there are other possibilities to excite bounded modes in a thin material slab, beyond the case where the material has a plasmalike electrical (or magnetic) response. Indeed, when the material has a large positive index of refraction it may support as well ultrasubwavelength guided modes. Based on this observation, in a recent work we have proposed a superlens made of a metamaterial with an extremely large positive index of refraction.[9] The metamaterial is formed by an ultradense array of nonconnected crossed metallic wires, which as demonstrated both theoretically and experimentally in Ref. 10, in the long-wavelength limit may mimic well the response of a continuous material with $\varepsilon \gg 1$. In particular, we have shown with numerical simulations in Ref. 9 that such metamaterial slab may enable subdiffraction imaging, effectively restoring part of the subwavelength spatial spectrum in the observation plane. The objective of this work is to confirm experimentally these potentials and give further insights about the properties of the system. It should be mentioned that even though arrays of metallic wires have been used before to transport the near field,[11] the imaging mechanism reported here is fundamentally different because it can effectively compensate for the decay of near field in the air regions.

The geometry of the considered lens is sketched in Fig. 1(a). It is formed by a stack of 308 printed circuit boards (ROGERS™ duroid-5880) with dielectric constant $\varepsilon_h = 2.2$, loss tangent $\tan\delta = 0.0009$, thickness $a/2 = 0.79$ mm, and area $D \times L = 182$ mm $\times 11.7$ mm. Each rectangular board is printed with an array of metallic strips tilted by $\pm 45°$ with respect to the $z$ direction. The metallic strips in consecutive boards are oriented along perpendicular directions. The width of the strips is $w_s = 0.247$ mm and the spacing between parallel strips is $a = 1.58$ mm. In Fig. 1(b) we depict the dispersion characteristic of the transverse electric (TE) guided

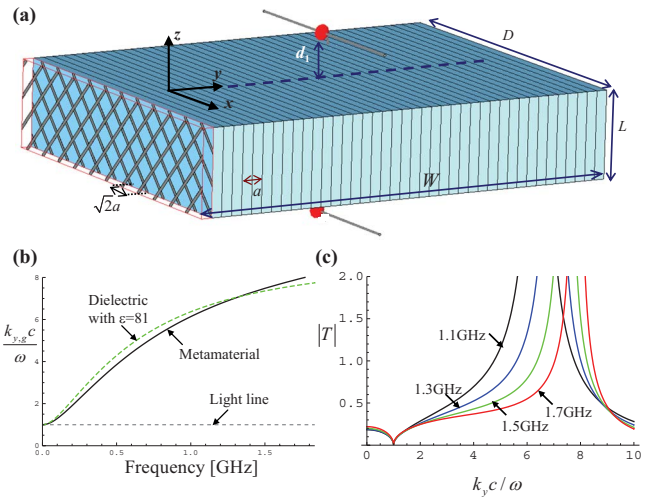


FIG. 1. (Color online) (a) Geometry of the metamaterial lens: a stack of dielectric slabs imprinted with an ultradense array of metallic strips with width $w_s$ and tilted by $\pm 45°$ with respect to the interfaces. (b) Dispersion characteristic of the TE-guided modes supported by a metamaterial slab with parameters $a/2 = 0.79$ mm, $L = 11.7$ mm, and $w_s = 0.247$ mm (solid black line). The electric field is along the $x$ direction and the direction of propagation is along $y$. (c) Amplitude of the transmission coefficient as a function of the normalized transverse wave vector component $k_y$ for different frequencies of operation. The curves of panels (b) and (c) were calculated using the full wave electromagnetic simulator CST Microwave Studio™ (Ref. 12).

 

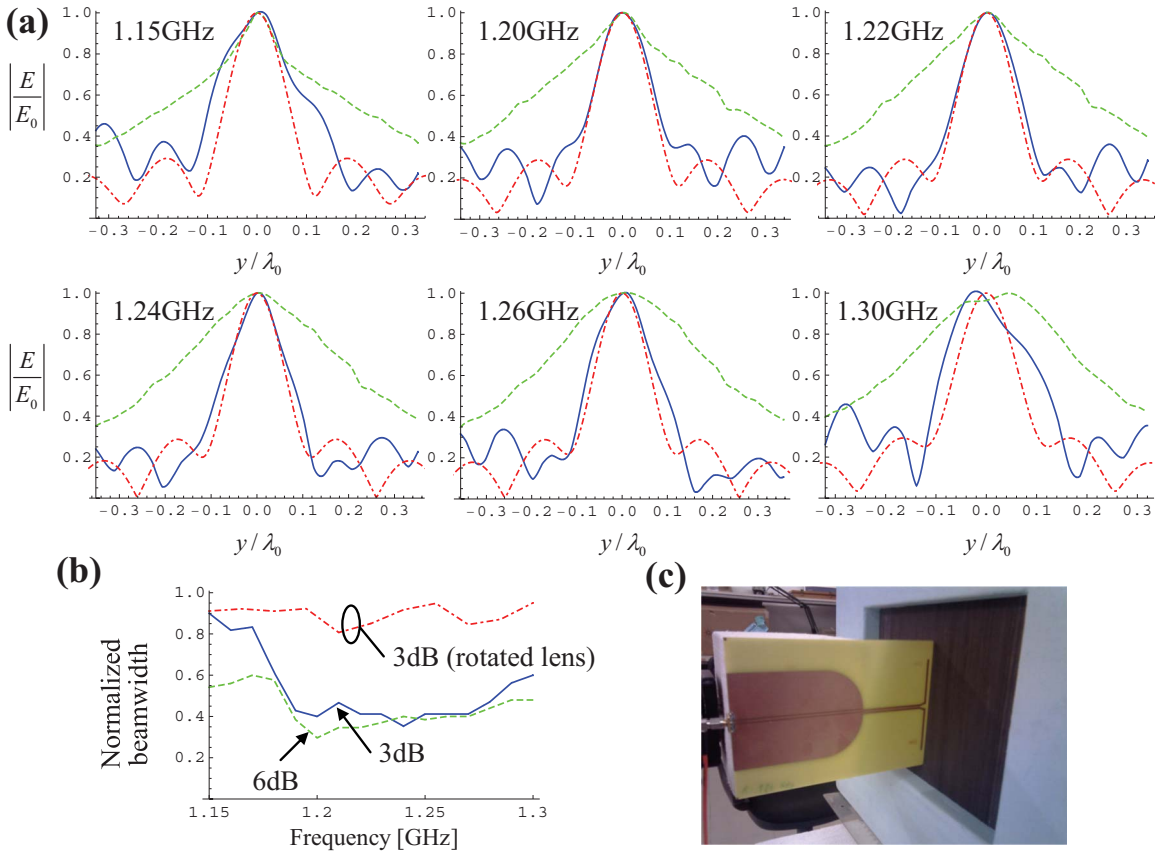


FIG. 2. (Color online) (a) Normalized electric field profiles at the image plane, for different frequencies of operation, when the source/probe antennas are printed dipole antennas resonant at 1.25 GHz in free space: solid blue line—measured results in the presence of the metamaterial lens; dashed green line—measured results in the absence of the lens; dot-dashed red line—theoretical field profile when the source is an ideal line of electric current (Ref. 9). The distance between the source/probe antennas and the lens is $d_1=d_2=0.5L$. (b) $BW_{\text{lens}}/BW_{free\text{-}space}$ as a function of frequency, where $BW_{\text{lens}}$ ($BW_{free\text{-}space}$) represents the beamwidth at the image plane in presence (absence) of the lens calculated with either a 3 dB (blue solid line) or 6 dB criterion (green dashed line). The dot-dashed red line was calculated in the same conditions as the solid blue line, except that the metamaterial lens was rotated by 90° so that the dipoles became orthogonal to the metallic strips. (c) Photo showing the fabricated prototype framed in a foam support, the source dipole, and its feeding circuitry (balun).

modes supported by a substrate with the same geometry but infinitely extended along the $x$ and $y$ directions. The wave number of the guided mode is $k_{y,g}$ and $\omega$ is the angular frequency in radians. Notwithstanding with the fact that the substrate is electrically very thin ($L=0.05\lambda_0$ at 1.25 GHz), it is seen that it supports guided modes associated with large values of $k_{y,g}c/\omega$ over a very broad frequency band. For comparison, we also show in Fig. 1(b) the dispersion characteristic of a dielectric slab with permittivity $\varepsilon=81$ and the same thickness as the metamaterial (dashed line).

When the substrate is placed in the vicinity of a source the guided modes may be resonantly excited, causing the enhancement of some components of the subwavelength spatial spectrum. Indeed, as shown in Fig. 1(c), the amplitude of the transfer function of the metamaterial slab (defined as the ratio $T=E_x|_{z=-L}/E_x|_{z=0}$ of the electric field at the output and input interfaces for plane-wave incidence with variation along $y$ of the type $e^{ik_y y}$) exhibits a resonant behavior when the transverse wave number of the incident wave is close to the propagation constant of the guided mode at the considered frequency, i.e., when $k_y \approx k_{y,g}$.

In order to demonstrate the super-resolution effect, we placed two printed dipole antennas (resonant frequency in free space is 1.25 GHz) at a distance $d_1=d_2=L/2$ from the fabricated prototype [Figs. 1(a) and 2(c)]. Microwave absorbers were positioned at the sides of the lens parallel to the dipoles to avoid diffraction from the edges. The prototype was designed to have optimal imaging characteristics around 1.2 GHz, which corresponds to the minimum of the transmission coefficient for normal incidence[9] [as seen in Fig. 1(c), the level of the transmission coefficient is very stable with respect to variations in frequency]. By scanning the position of the probe antenna along the $y$ direction, we measured the profile of the electric field at the image plane for different frequencies of operation [solid lines in Fig. 2(a)]. In the same plots we show the measured field profiles (dashed lines) when the superlens is removed, keeping the total propagation distance in the air regions invariant (thus the distance between the source and probe is decreased two times). Notwithstanding with the greater proximity between the antennas, it is seen that when the lens is absent the beamwidth becomes significantly broader, especially around 1.25

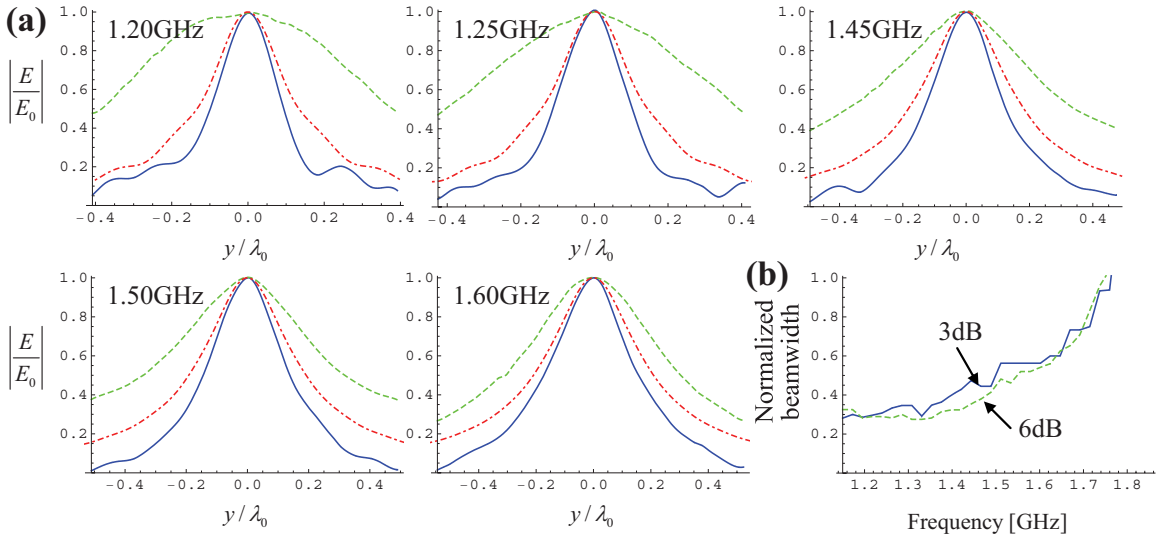


FIG. 3. (Color online) (a) Similar to Fig. 2(a), except that the set of printed dipoles used in this example is resonant at 1.5 GHz in free space and the dipoles are at a distance $d_1=d_2=1.1L$ from the lens. (b) Similar to Fig. 2(b) but for the second set of dipoles.

GHz, where the half-power (−3 dB) beamwidth (HPBW) has a minimum in the presence of the lens. At 1.24 GHz the HPBW is about $0.12\lambda_0$, well below the conventional diffraction limit. The dot-dashed lines in Fig. 2(a) represent the theoretical electric field profile when the metamaterial lens is infinitely extended along the $x$ and $y$ directions and is illuminated by an infinitely long electric line source. The results were obtained using the analytical model reported in Ref. 9 and supposing that the metallic strips can be modeled as wires with an equivalent radius $R=w_s/\pi$. Despite the fact that such configuration is significantly different from the actual experimental setup, the agreement between the dot-dashed and solid lines is quite reasonable, especially in the range 1.20–1.26 GHz, demonstrating that the theory of Ref. 9 may be used to estimate the response of the lens when the source is a dipole antenna. However, it should be emphasized that such theory is only a very rough description of the considered system because, in general, the electric field profile created by the dipole antenna at the input interface may differ substantially from the field profile created by an ideal line source and, more importantly, such simplistic theory neglects the coupling between the antenna and the lens, which may change the radiation properties of the antenna in some complicated manner. Such coupling is increasingly important when the electrical distance between the source and the lens is small (i.e., at lower frequencies). This may explain the deterioration of the imaging properties at 1.15 GHz. On the other hand, it is also seen in Fig. 2(a) that the field profile at the image plane has some oscillations at 1.30 GHz, even in the absence of the lens. This effect is clearly due to the coupling between the source/probe dipoles (the dipoles resonate in free space at 1.25 GHz), which perturbs the electric field profile at the input interface and limits the performance of the system, especially when the electrical distance between the dipoles is relatively small as in this example.

The measured ratio between the $S_{21}$ parameters referred to the connectors of the source and receiving dipole antennas when the two dipoles are face to face, $S_{21}|_{\text{in presence of the lens}}/S_{21}|_{\text{in absence of the lens}}$, is about 1.1 at 1.24 GHz and varies less than 20% in the frequency interval 1.15–1.30 GHz. This important result clearly shows that our near-field imaging system effectively redirects a large portion of the incoming energy to the image plane, without changing appreciably the peak level of the transmitted field, and demonstrates the robustness of the imaging mechanism under study in terms of transmission efficiency.

In Fig. 2(b), the solid line represents the ratio between the measured HPBW in presence of the lens and the HPBW in free space. At the design frequency this ratio is close to 0.5, clearly proving that the presence of the superlens boosts the resolution of the image. In the same figure, we also plot the normalized beamwidth determined by the −6 dB point (dashed line), being the results qualitatively similar to those obtained using the −3 dB criterion. As a control experiment, we have rotated the lens by 90° so that the metallic strips became orthogonal to the dipole antennas. In these circumstances, the strips interact weakly with the field radiated by the source, and thus it is expected that the metamaterial substrate behaves nearly in the same manner as a solid dielectric block with the same permittivity ($\varepsilon_h=2.2$) as the host material, and thus no improvement in the resolution is expected. The measured normalized beamwidth for this scenario is also depicted in Fig. 2(b) (dot-dashed line), confirming that when the substrate is rotated the image resolution becomes limited by diffraction.

It is important to mention the resolution of our system is not directly determined by the wavelength of radiation $\lambda=\lambda_0/n$ inside the metamaterial slab, being $n$ the effective index of refraction of the slab [from Fig. 1(b), $n$ may be roughly estimated as $n=\sqrt{81}$]. Specifically, the resolution of our system is not determined by $\lambda/2$, as it would happen if the source of radiation were placed *inside* the metamaterial slab. In our setup the dipole antennas are placed in the air region and at a significant distance (in the near-field context) from the lens. Indeed, the imaging mechanism is not directly based on the shortening of the wavelength inside the lens but

instead on the resonant excitation of guided modes and amplification of the subwavelength spectrum.

As discussed above, the quality of imaging depends on the radiation characteristics of the source/probe antennas, which in this type of near-field systems may be quite sensitive to the presence of the metamaterial lens. Thus the radiation characteristic of the source in the presence of the lens may differ from the radiation characteristic in free space. In order to demonstrate that the proposed system may have a broadband response, we have excited the same lens with a second set of dipole antennas tuned to 1.5 GHz. Increasing the resonant frequency of the dipoles helps reducing the coupling to the metamaterial substrate and thus the radiation characteristics of the antennas may be less affected by the presence of the lens. The field profiles measured with this second set of antennas are shown in Fig. 3 for different frequencies, together with the measured HPBW (for a fixed propagation distance in air: $d=d_1+d_2$). The distance between the dipoles and the lens for this set of measurements was $d_1=d_2=1.1L$. The results show that even though the imaging properties are progressively deteriorated as the frequency increases (as expected since the electrical distance between the source/probe antennas and the lens increases with frequency), the range where the super-resolution effect is observed can be quite significant, exceeding 25% of the operation frequency. As in the previous example, the optimal imaging occurs around 1.2 GHz but since the coupling between the source/probe antennas and the metamaterial is weaker (because both the resonant frequency of the antennas and $d_1$ and $d_2$ are larger) the imaging bandwidth for the second set of dipoles is better than that for the first set. We have also measured the electric field profile at 1.25 GHz (using the set of dipoles tuned to 1.5 GHz) and for different distances $d_2$ of the probe antenna to the lens, keeping the distance between the source and the lens fixed ($d_1=1.1L$). The results of Fig. 4 show that the transmitted beam remains significantly narrower than the beam radiated by the source in free space, even for large values of $d_2$.

In conclusion, we have experimentally demonstrated that a dense array of crossed metallic strips may enable imaging with resolution well below the diffraction limit over a very broad bandwidth and with good transmission efficiency. The imaging mechanism is based on the excitation of guided modes in a nonresonant metamaterial with a large index of refraction. It was demonstrated that the presence of the superlens boosts the resolution of the system, as if the source and image planes were effectively closer, whereas in reality the total physical distance between the source and the image planes increases significantly in presence of the superlens. In this sense, the "electromagnetic thickness" of the metamaterial is effectively negative. A scaled prototype of the same lens may have essentially the same properties at terahertz frequencies.[9] Due to its intrinsically broadband nature, this type of subdiffraction imaging systems (with bandwidths exceeding 25%) may be competitive with solutions based on either photonic crystals[8] or materials with negative parameters[1] which are typically very narrow-band proposals. We envision that the proposed system may have applications in sensing, lithography, and radiofrequency identification systems.

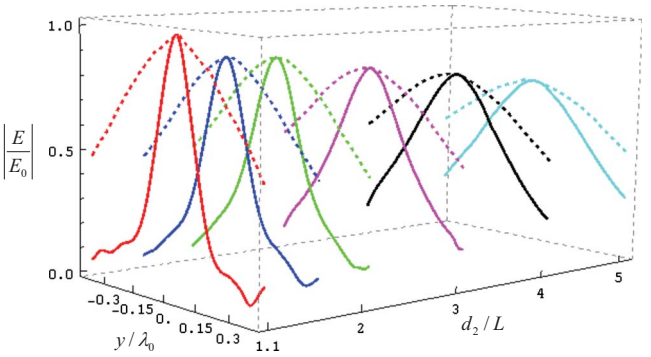


FIG. 4. (Color online) Normalized electric field profiles as a function of the distance $d_2$ of the probe antenna to the lens interface. The results were measured at 1.25 GHz using the second set of dipoles (tuned for 1.5 GHz). The distance between the source antenna and the lens is kept fixed: $d_1=1.1L=1.3$ cm. The solid lines represent the measured results in the presence of the lens, whereas the dashed lines represent the measured results when the lens is absent.

The authors gratefully acknowledge technical support from Carlos Brito, Vasco Fred, and António Almeida.

[1] J. B. Pendry, Phys. Rev. Lett. **85**, 3966 (2000).
[2] N. Fang, H. Lee, C. Sun, and X. Zhang, Science **308**, 534 (2005).
[3] M. J. Freire, R. Marques, and L. Jelinek, Appl. Phys. Lett. **93**, 231108 (2008).
[4] Z. Liu, H. Lee, Y. Xiong, C. Sun, and X. Zhang, Science **315**, 1686 (2007).
[5] I. I. Smolyaninov, Y.-J. Hung, and C. C. Davis, Science **315**, 1699 (2007).
[6] R. Merlin, Science **317**, 927 (2007); A. Grbic, L. Jiang, and R. Merlin, *ibid.* **320**, 511 (2008).
[7] I. I. Smolyaninov, C. C. Davis, J. Elliott, G. A. Wurtz, and A. V. Zayats, Phys. Rev. B **72**, 085442 (2005).
[8] C. Luo, S. G. Johnson, J. D. Joannopoulos, and J. B. Pendry, Phys. Rev. B **68**, 045115 (2003).
[9] M. G. Silveirinha, C. A. Fernandes, and J. R. Costa, Phys. Rev. B **78**, 195121 (2008).
[10] M. G. Silveirinha, C. A. Fernandes, J. R. Costa, and C. R. Medeiros, Appl. Phys. Lett. **93**, 174103 (2008); M. G. Silveirinha and C. A. Fernandes, Phys. Rev. B, **78**, 033108, (2008).
[11] P. A. Belov, Y. Hao, and S. Sudhakaran, Phys. Rev. B **73**, 033108 (2006); G. Shvets, S. Trendafilov, J. B. Pendry, and A. Sarychev, Phys. Rev. Lett. **99**, 053903 (2007); M. G. Silveirinha and N. Engheta, *ibid.* **102**, 103902 (2009).
[12] CST Microwave Studio™ 2008, www.cst.com